Equivalent static wind loads for structures with non-proportional damping

N. Blaise & V. Denoël
Department of Architecture, Geology, Environment and Constructions
Structural Engineering Division
University of Liège, Liège, Belgium

T. Canor
F.R.S.-FNRS, National Fund for Scientific Research
University of Liège, Liège, Belgium

ABSTRACT: Usually, wind structural design is often carried out by a recourse to the concept of equivalent static wind loads. The main advantage of such loadings is to reproduce, with static analyses, the same extreme structural responses as those resulting from a formal buffeting analysis. This paper proposes an asymptotic method for the computation of equivalent static wind loads for structures with non-proportional damping in a modal framework. This method is based on recent results obtained with asymptotic expansion of the modal transfer matrix of such structures. The method is illustrated on a wind-sensitive high building mitigated with a tuned mass damper (TMD) or a tuned liquid column damper (TLCD). Each damping device produces a different level of coupling allowing to study the convergence of the proposed method. For a similar level of mitigation, the TMD introduces more coupling than the TLCD does. Relative errors on structural responses (displacements, internal forces) are critically analysed.

1 INTRODUCTION

Over the last years, methods have been derived to compute equivalent static wind loads for structures with quasi-static (Davenport 1967, Holmes 1988, Kasperski 1992) or resonant behaviour (Holmes 1996, Zhou, Gu, & Xiang 1999, Chen & Kareem 2001, Blaise & Denoël 2013), analysed in nodal or modal basis. Equivalent static wind loads are derived to produce, with static analyses, the same extreme structural responses as those obtained with formal dynamic analyses. In the modal basis, such static loadings are defined as weighted combinations of inertial loads. An inertial load statically applied to the structure produces a deflection affine to the corresponding mode shape. The control of dynamic response of wind-sensitive structure such as wide-span roofs or bridges and high-rise buildings may be achieved using damping devices, e.g. tuned mass damper as well as tuned liquid dampers. These damping devices are source of non-proportional damping and consequently, the modal damping matrix and the modal transfer matrix are no longer diagonal. In this case, the dynamic analysis in the modal basis enables to reduce the size of the system, M-modes $\ll N$-degrees of freedom, but not to decoupled the modal equations. Rayleigh (1945) has proposed a decoupling approximation that neglects these off-diagonal elements of the modal damping matrix due to their relative smallness compared with the diagonal ones. Recently, an asymptotic expansion of the modal transfer matrix has been proposed by Denoël & Degée (2009) in a deterministic framework and then extend to a stochastic context (Canor, Blaise, & Denoël 2012), that enables to avoid full transfer matrix inversions for all frequencies.

For structures with non-proportional damping, this paper further extends the formulation of the asymptotic expansion to the weighting coefficients necessary to derive equivalent static wind loads with the inertial loads. The proposed method is formulated with the by-products resulting from the application of the asymptotic expansion of the modal transfer matrix.

The method is illustrated with a realistic example and a detailed analysis of the asymptotic convergence of both modal amplitudes and weighting coefficients of the inertial loads is performed.

2 BUFFETING WIND ANALYSIS

We consider a stationary Gaussian random loading $\mathbf{p}_{tot}(t)$, representing wind actions, although the concepts could be generalized to other loadings. For con-

venience the loading is split into a mean part $\boldsymbol{\mu}_p$ and a fluctuating part $\mathbf{p}(t)$

$$\mathbf{p}_{tot} = \boldsymbol{\mu}_p + \mathbf{p}. \tag{1}$$

The dynamic motion $\mathbf{x}(t)$ of a linear structure loaded by this random excitation, in the nodal basis, is obtained by solving the equation of motion

$$\mathbf{M}\ddot{\mathbf{x}} + \mathbf{C}\dot{\mathbf{x}} + \mathbf{K}\mathbf{x} = \mathbf{p} \tag{2}$$

where $\mathbf{M}$, $\mathbf{C}$ and $\mathbf{K}$ are $N \times N$ mass, damping and stiffness matrices, respectively. Contributions to the damping matrix are the structural $\mathbf{C}_s$, concentrated $\mathbf{C}_c$ (due to damping devices) and aerodynamic damping $\mathbf{C}_a$ matrices. The structural responses $\mathbf{r}(t)$ (nodal displacements, internal forces or reactions) are considered here to be expressed as linear combinations of the nodal displacements

$$\mathbf{r} = \mathbf{O}\mathbf{x} \tag{3}$$

where $\mathbf{O}$ is a matrix of influence coefficients, typically known from the FE model. The structural response of a given linear dynamic system can be computed using a small number M of normal modes of vibrations ($M \ll N$) characterized by mode shapes $\boldsymbol{\Phi}$ (Clough & Penzien 1993). These modes are normalized to have unit generalized masses. Using the modal superposition principle, the equation of motion (2) is written as

$$\ddot{\mathbf{q}} + \mathbf{D}\dot{\mathbf{q}} + \boldsymbol{\Omega}\mathbf{q} = \mathbf{g} \tag{4}$$

where $\mathbf{q}(t)$ ($\mathbf{x} = \boldsymbol{\Phi}\mathbf{q}$) is the vector of modal coordinates, $\mathbf{g}(t) = \boldsymbol{\Phi}^{\mathrm{T}}\mathbf{p}(t)$ is the vector of generalized forces, $\boldsymbol{\Omega}$ is a diagonal matrix containing generalized stiffnesses (equal, in this case, to the squared circular frequencies) and $\mathbf{D} = \boldsymbol{\Phi}^{\mathrm{T}}\mathbf{C}\boldsymbol{\Phi}$ is the modal damping matrix. The frequency domain formulation of the equation of motion in the modal basis is obtained by a side-by-side Fourier Transform of (4)

$$\mathbf{Q} = \mathbf{H}\,\mathbf{G} \tag{5}$$

where $\mathbf{Q}(\omega)$ and $\mathbf{G}(\omega)$ are respectively the Fourier transforms of $\mathbf{q}$ and $\mathbf{g}$. The modal transfer matrix $\mathbf{H}(\omega)$ is defined by

$$\begin{aligned} \mathbf{H} &= \left(\boldsymbol{\Omega} - \omega^2\mathbf{I} + i\omega\left(\mathbf{D}_d + \mathbf{D}_o\right)\right)^{-1} \\ &= \left(\mathbf{I} + \mathbf{H}_d\mathbf{J}_o\right)^{-1}\mathbf{H}_d \end{aligned} \tag{6}$$

where $\mathbf{D}_d$ and $\mathbf{D}_o$ are built as $D_{d,ij} = D_{ij}\delta_{ij}$ (diagonal elements) and $D_{o,ij} = D_{ij}(1-\delta_{ij})$ (off-diagonal elements) where δ_{ij} denotes the Kronecker-delta function and $\mathbf{H}_d(\omega) = \left(\boldsymbol{\Omega} - \omega^2\mathbf{I} + i\omega\mathbf{D}_d\right)^{-1}$, $\mathbf{J}_o(\omega) = i\omega\mathbf{D}_o$. The asymptotic expansion of the modal transfer matrix (6) for small off diagonal elements (Denoël & Degée 2009) gives

$$\mathbf{H}_k = \mathbf{H}_d + \sum_{i=1}^{k}\left(-1\right)^i\left(\mathbf{H}_d\mathbf{J}_o\right)^i\mathbf{H}_d \tag{7}$$

where k is the approximation order of the transfer function. The psd matrix of the modal coordinates $\mathbf{S}^{(q)}(\omega)$, is obtained by

$$\mathbf{S}^{(q)} = \mathbf{H}\mathbf{S}^{(g)}\mathbf{H}^* \tag{8}$$

where the superscript * denotes the conjugate transpose operator and where $\mathbf{S}^{(g)}(\omega)$ is the psd matrix of the generalized Gaussian forces. The k^{th} approximation of the psd matrix of the modal displacements (8) is obtained by

$$\mathbf{S}^{(q_k)} = \mathbf{S}^{(q_d)} + \sum_{i=1}^{k}\boldsymbol{\Delta}\mathbf{S}^{(q_i)};\ \mathbf{S}^{(q_d)} = \mathbf{H}_d\mathbf{S}^{(g)}\mathbf{H}_d^* \tag{9}$$

where $\mathbf{S}^{(q_d)}$ $(k=0)$ is the psd matrix in the uncoupled system and the successive correction terms $\boldsymbol{\Delta}\mathbf{S}^{(q_i)}$ are expressed in a general recurrence relation

$$\begin{aligned} \boldsymbol{\Delta}\mathbf{S}^{(q_i)} &\overset{i=1}{=} -\left(\mathbf{H}_d\mathbf{J}_o\mathbf{S}^{(q_d)} + \mathbf{S}^{(q_d)}\mathbf{J}_o^*\mathbf{H}_d^*\right) \\ &\overset{i>1}{=} -\left(\mathbf{H}_d\mathbf{J}_o\boldsymbol{\Delta}\mathbf{S}^{(q_{i-1})} + \boldsymbol{\Delta}\mathbf{S}^{(q_{i-1})}\mathbf{J}_o^*\mathbf{H}_d^*\right) \\ &\quad -\mathbf{H}_d\mathbf{J}_o\boldsymbol{\Delta}\mathbf{S}^{(q_{i-2})}\mathbf{J}_o^*\mathbf{H}_d^* \end{aligned} \tag{10}$$

with $\boldsymbol{\Delta}\mathbf{S}^{(q_0)} = \mathbf{S}^{(q_d)}$. In the following, the covariance matrix $\mathbf{C}^{(q_k)}$ of the modal coordinates, is calculated by integration (along the circular frequencies) of the corresponding psd matrix

$$\mathbf{C}^{(q_k)} = \int_{-\infty}^{+\infty}\mathbf{S}^{(q_k)}\,d\omega = \mathbf{C}^{(q_d)} + \sum_{i=1}^{k}\boldsymbol{\Delta}\mathbf{C}^{(q_i)} \tag{11}$$

where k denotes one of the aforementioned methods, namely (i) the exact approach ($q_\infty \equiv q$), (ii) the decoupling approximation ($q_0 \equiv q_d$), (iii) the proposed approximation with k correction terms.

The structural design needs envelope values (minimum and maximum) of the structural responses which are computed here as expected values of extrema on 10-minute observation windows. The envelope $(\mathbf{r}^{min}, \mathbf{r}^{max})$ is defined as

$$\mathbf{r}^{k,min} = -\mathbf{g}^k \circ \boldsymbol{\sigma}^{r_k}\ ;\ \mathbf{r}^{k,max} = \mathbf{g}^k \circ \boldsymbol{\sigma}^{r_k} \tag{12}$$

where $\boldsymbol{\sigma}^{r_k}$ is the standard deviation of the structural response, $\mathbf{g}^k$ is the peak factor derived from Rice's formula (Rice 1945) and $\circ$ denotes the Hadamard product operator. The k^{th} approximation of standard deviations of the structural responses are derived from the corresponding covariance matrix of the modal displacements using

$$\boldsymbol{\sigma}^{r_k} = \sqrt{diag\left(\boldsymbol{\Upsilon}\mathbf{C}^{(q_k)}\boldsymbol{\Upsilon}^{\mathrm{T}}\right)} \tag{13}$$

where $\boldsymbol{\Upsilon} = \mathbf{O}\boldsymbol{\Phi}$ is the matrix of modal structural responses with υ_{im} the value of the i^{th} structural response in the m^{th} mode and *diag* is a matrix operator that keeps only the diagonal of the matrix. For the

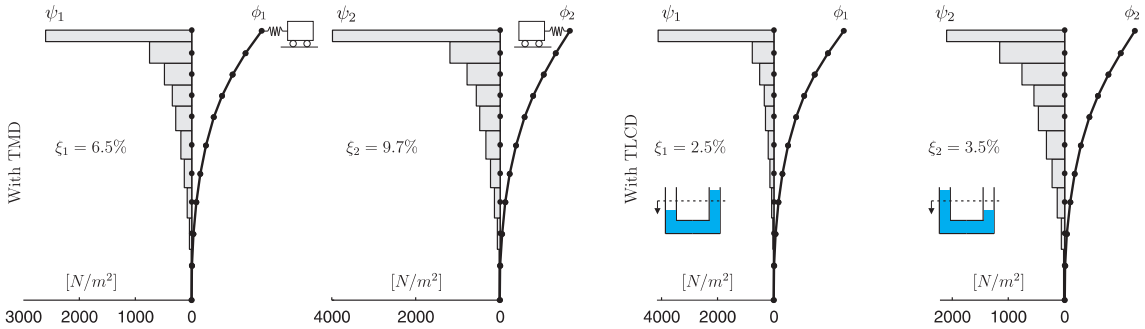

Figure 1: First two modal horizontal components (normalized to have a top displacement equal to 10 cm) and inertial horizontal forces per wind area. Each circle represents the nodes of the FE model. For each figure, the left and the right illustrate results for the structure with TMD and with TLCD, respectively.

structural design, the maximum value of the j^{th} structural response is given by the following formula with a CQC approach:

$$r_j^{k,max} = g_j^k \left(\sum_{m=1}^{M} \sum_{n=1}^{M} \upsilon_{jm} \upsilon_{jn} \sigma_{mn}^{q_k} \right)^{1/2} = g_j^k \frac{\sum_{m=1}^{M} \sum_{n=1}^{M} \upsilon_{jm} \upsilon_{jn} \sigma_{mn}^{q_k}}{\sigma_j^{r_k}} \quad (14)$$

where $\sigma_{mn}^{q_k} = \sigma_{mn}^{q_d} + \sum_{i=1}^{k} \Delta\sigma_{mn}^{q_i}$ is the covariance between the m^{th} and n^{th} modes, formally obtained with (11), or more efficiently with an approximate relation (Denoël 2009).

3 EQUIVALENT STATIC WIND LOAD

The static analysis under an equivalent static wind load (ESWL) $\mathbf{p}_j^{e,k}$ associated with the j^{th} response reproduces the maximum dynamic response $r_j^{k,max}$ obtained with a classical buffeting analysis:

$$\mathbf{r}_j^{e,k} = \mathbf{A}\mathbf{p}_j^{e,k} \text{ with } r_{jj}^{e,k} = r_j^{k,max} \quad (15)$$

where $\mathbf{r}_j^{e,k}$ is a vector of structural responses under the j^{th} ESWL and $\mathbf{A} = \mathbf{O}\mathbf{K}^{-1}$ is a matrix of influence coefficients.

Inertial forces are defined as inertial load excitation that produce the dynamic displacement from (2) under a static analysis, i.e.

$$\mathbf{x} = \mathbf{\Phi}\mathbf{q};\ \mathbf{K}\mathbf{x} = \mathbf{\Psi}\mathbf{q} \quad (16)$$

where $\mathbf{\Psi} = \mathbf{K}\mathbf{\Phi}$ is the matrix of inertial forces with $\boldsymbol{\psi}_m$ the inertial force associated with the m^{th} modal shape. Chen & Kareem (2001) have proposed to derive ESWL from combinations of these inertial forces using adequate weighting coefficients.

What is discussed next is the formulation of these weighting coefficients with corrections terms if the system is coupled. The matrix of modal structural responses may be also computed with the inertial forces as

$$\mathbf{\Upsilon} = \mathbf{A}\mathbf{\Psi};\ \boldsymbol{\upsilon}_{jm} = \mathbf{a}_j \boldsymbol{\psi}_m, \quad (17)$$

and the introduction of (17) into (14) gives

$$r_j^{k,max} = a_j g_j^k \sum_{m=1}^{M} \left(\frac{\sum_{n=1}^{M} \upsilon_{jn} \sigma_{mn}^{q_k}}{\sigma_j^{r_k}} \right) \boldsymbol{\psi}_m = a_j g_j^k \sum_{m=1}^{M} \left[\frac{\sigma_j^{r_d}}{\sigma_j^{r_k}} W_{jm}^d \boldsymbol{\psi}_m + \sum_{i=1}^{k} \Delta W_{jm}^i \boldsymbol{\psi}_m \right]$$

where the weighting factors W_{jm}^d and ΔW_{jm}^i are expressed by

$$W_{jm}^d = \frac{\sum_{n=1}^{M} \upsilon_{jn} \sigma_{mn}^{q_d}}{\sigma_j^{r_d}};\ \Delta W_{jm}^i = \frac{\sum_{n=1}^{M} \upsilon_{jn} \Delta\sigma_{mn}^{q_i}}{\sigma_j^{r_k}}.$$

The k^{th} approximation of the static loading, $\mathbf{p}^{e,k}$, is described as a summation of two contributions: (a) a scaling of the equivalent loading that would be obtained if the system was uncoupled, $\mathbf{p}^{e,d}$ and (b) a corrective equivalent loading, $\Delta\mathbf{p}_j^k$, resulting from the non-proportionality of damping:

$$\mathbf{p}_j^{e,k} = \left[\alpha_j^k \mathbf{p}_j^{e,d} + \Delta\mathbf{p}_j^{e,k} \right] = g_j^k \sum_{m=1}^{M} W_{jm}^k \boldsymbol{\psi}_m \quad (18)$$

$$\mathbf{p}_j^{e,d} = g_j^d \sum_{m=1}^{M} W_{jm}^d \boldsymbol{\psi}_m \quad (19)$$

$$\Delta\mathbf{p}_j^{e,k} = g_j^k \sum_{m=1}^{M} \sum_{i=1}^{k} \Delta W_{jm}^i \boldsymbol{\psi}_m \quad (20)$$

where $\alpha_j^k = \left(g_j^k \sigma_j^{r_d}\right) / \left(g_j^d \sigma_j^{r_k}\right)$ is a scaling coefficient and the k^{th} approximation of the weighting coefficients W_{jm}^k is derived from

$$W_{jm}^k = \alpha_j^k W_{jm}^d + \sum_{i=1}^{k} \Delta W_{jm}^i \quad (21)$$

which well extends the formulation $W_{jm}^k = W_{jm}^d$ corresponding to the case where modal coupling is neglected. Notice also that α_j degenerates in $\alpha_j = 1$ for $k = 0$.

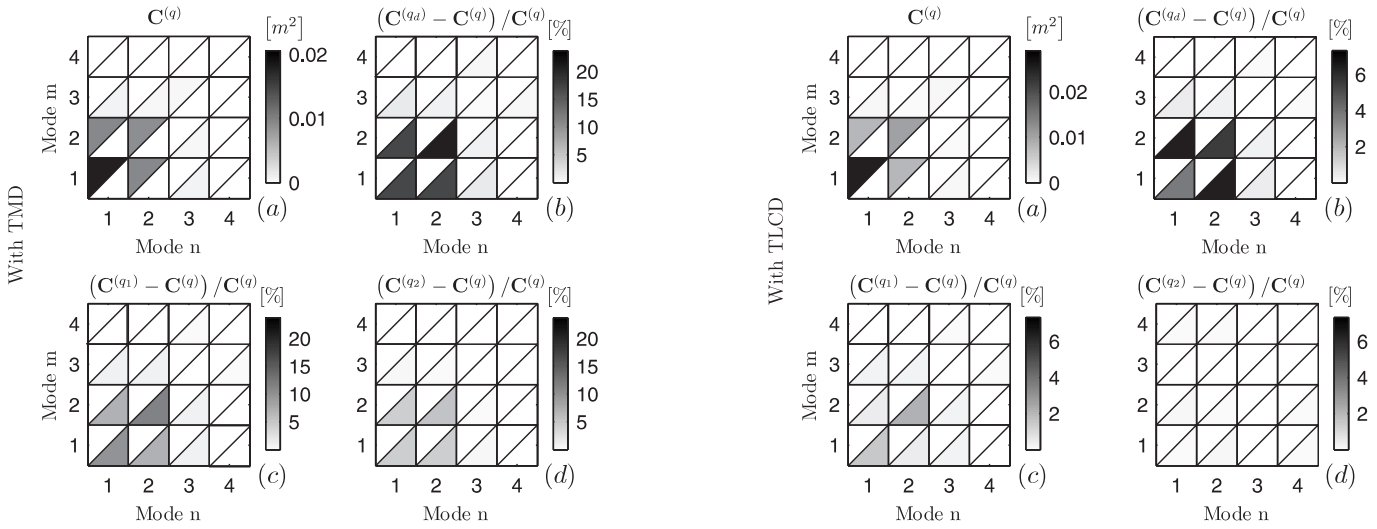

Figure 2: (a) Exact covariance matrix of the modal coordinates $\mathbf{C}^{(q)}$ (b) and relative error for different approximations $\mathbf{C}^{(q_d)}$, (c) $\mathbf{C}^{(q_1)}$ and (d) $\mathbf{C}^{(q_2)}$. Relative errors are expressed with respect to $\mathbf{C}^{(q)}$. For each square, the upper left corner correspond to positive value and the lower right corner to negative value.

4 ILLUSTRATION

A 76-story, 306 m tall building is analysed under wind actions. This structure is a numerical example used in (Xu, Samali, & Kwok 1992) to study the mitigation of the along-wind response of structures using a tuned liquid column damper (TLCD) instead of a tuned mass damper (TMD). The structural model is a 10 lumped-mass cantilever model with 11 nodes and the finite element (FE) model is an assembly of classical 2-D beam elements with two DOFs per node (rotation and horizontal displacement). The proposed method is illustrated on this structure, with each damping device, keeping the first four modes for the modal analysis. The TMD or the TLCD are connected to the top floor of the building and are tuned to match the fundamental frequency of the structure. Both structures (with TMD or TLCD) have similar natural frequencies equal to 0.16, 0.19, 0.57 and 1.33 Hz. Figure 1 depicts the horizontal components of the first two modes and the corresponding inertial forces. A one-dimensional Gaussian velocity turbulence field is considered. The longitudinal turbulent component v of the velocity field is modeled by the spectrum of longitudinal turbulence proposed by Davenport (1961). The spanwise coherence function of v between two points of the tower separated by a height l is modelled by a decreasing exponential. Structural, TMD, TLCD and wind load spectrum data are not reported here for sake of conciseness but may be found in (Xu, Samali, & Kwok 1992). In a unidimensional turbulence model, a linearized expression of the zero-mean fluctuating applied force at the i^{th} level $p_i(t)$ is adopted as

$$p_i = C_{a,i} v_i \tag{22}$$

in which $C_{a,i}$ reads

$$C_{a,i} = \frac{\overline{W}_{10}}{\overline{V}_{10}} \sqrt{6K_0} C_d A_i \left(\frac{H_i}{10}\right)^{\alpha} \tag{23}$$

where $\overline{W}_{10}$, $\overline{V}_{10}$ K_0, C_d, A_i, H_i and α are the mean wind pressure at 10 meters, the mean wind velocity at 10 meters, the surface drag coefficient, the drag coefficient, the surface exposed to wind, the height of the i^{th} level and the exponent coefficient, respectively. The aerodynamic damping is taken into account and therefore a diagonal aerodynamic damping matrix $\mathbf{C}_a$ is added to the structural $\mathbf{C}_s$ and concentrated damping $\mathbf{C}_c$ to constitute the total damping matrix $\mathbf{C} = \mathbf{C}_s + \mathbf{C}_c + \mathbf{C}_a$. The index of diagonality (see Horn & Johnson 1945) defined as $\rho(\mathbf{D}) = \sigma\left[\mathbf{D}_d^{-1}\mathbf{D}_o\right]$ where $\sigma[\cdot]$ is the spectral radius is an indicator of the diagonal dominance of $\mathbf{D}$. A low value indicates that the off-diagonal terms are small compared to the diagonal ones. The structure without damping device but considering the non proportional aerodynamic damping has an index equal to 0.02 and the classical decoupling approximation may be applied. Because of the TMD (resp. TLCD) the index of diagonality increases to 1.72 (resp. 1.03) and the classical decoupling approximation can not be formulated anymore. A larger diagonal index for the structure with TMD rather than with the TLCD, indicates that the solution with the decoupling approximation has a larger discrepancy with the reference solution ($k = \infty$). The reference covariance matrix ($k = \infty$) of modal coordinates and the relative error for the different approximations are represented in Figure 2. Concerning modes 1 and 2 the proximity of their natural frequencies and the similarities of mode shapes induce dynamic coupling (Denoël 2009) and high modal correlation coefficients equal to 0.78 and 0.5, respectively with TMD or TLCD. Figure 2-(b) on the left indicates that neglecting off-diagonal terms of the damping matrices, induces a maximum error of -23% on the variance of mode 2. The proposed method with first and second order correction terms offers a reduction of this error down to -14% and -6%, respectively. Figure 2-(b) on the right indicates that the de-

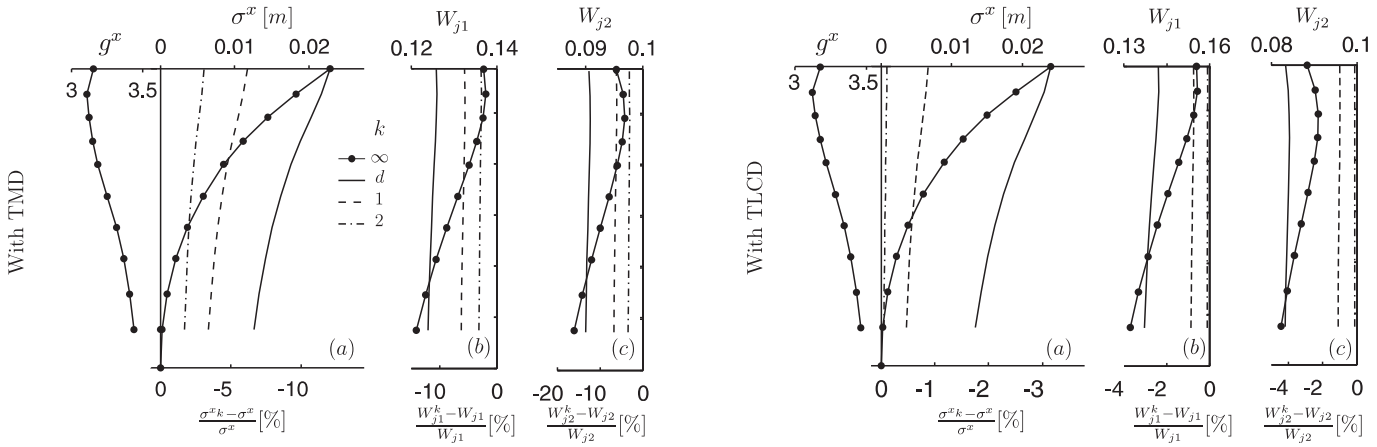

Figure 3: Results for the structural displacements. The upper axis, corresponding to reference values ($k = \infty$), is associated with lines with circles. The lower axis, corresponding to relative errors, is associated with solid ($k = d$), dashed ($k = 1$) and dashed-dot ($k = 2$) lines. (a) On the left, the peak factors and on the right standard deviations. (b) Weighting coefficients of the first and (c) the second inertial force for each structural displacement.

coupling approximation, induces a maximum error of -7.3% on the covariance between mode 1 and 2. Addition of the first and second correction terms reduces this error down to -1.9% and -0.25%, respectively. For the three approximations, the errors are the most significant for the group of correlated modes (1 and 2). Comparison of these relative errors on the covariance matrix for two levels of non proportionality (quantified by $\rho(\mathbf{D})$) shows that the proposed method with second order (or more) correction terms have to be considered for the structure with TMD while only the first correction term may be sufficient for the structure with TLCD. Figure 3-(a) depicts the peak factors and standard deviations of nodal horizontal displacements obtained with the reference approach. On the right is also represented the relative errors for each displacement, for the first three approximations. The decoupling approximation leads to underestimations of the displacements up to -12% (resp. -3%) for the structure with TMD and TLCD. With only the first correction term of the proposed method, these extreme underestimations are divided by two (resp. by three). The second order approximation provides underestimations less than -3 % (resp. $\simeq 0\%$) and therefore this order of approximation is used for the computation of equivalent static wind loads. In both cases, for the decoupling approximation, relative errors on the peak factors are less than 2% and therefore are not represented. For each structural displacement, Figure 3-(b) and -(c) illustrate the weighting coefficients for the first and second inertial force, respectively. As expected, the relative errors and the convergence are similar to those associated with the evaluation of the standard deviations of the structural displacements. The structural displacement at the top is chosen for the illustration of the proposed method. Figure 4-(a) depicts the reference equivalent static wind loads ($k = \infty$) and those obtained with the decoupling approximation ($k = 0$) and with second order correction terms ($k = 2$). Underestimations of the reference loadings occur with the decoupling approximation and a second order approximation is necessary to correctly fit the reference static loadings. The largest underestimations of the loadings are located at the top of the structure. Figure 4-(b) illustrates the static displacement under the reference ESWL. For the structure with the TMD, the decoupling approximation produces underestimations up to -12% while with the first two correction terms, relative errors are reduced down to -3%. Figure 4-(c) shows the static bending moments under the reference ESWL. The decoupling approximation produces underestimations up to -21% which are reduced to -1.5% with the first two corrections terms. For the TLCD, as expected, relative errors are smaller than those obtained for the structure with TMD. Levels of errors for the static displacements and static bending moments are similar to those reported for the weighting coefficients, see Figure 3.

5 CONCLUSIONS

High-rise buildings may be excited by the wind loading resulting in unacceptable level of displacements, internal forces or stresses. For such cases, among other solutions, damping devices are usually used to mitigate the wind response of such structures. These damping devices may be tuned mass or liquid column dampers and introduce non-proportional damping. A new method consisting in the asymptotic expansion of the modal transfer matrix enables to avoid full transfer matrix inversion. This work developed further the method for the establishment of equivalent static wind loads. The new method is illustrated with a 306 m tall building tower with (a) a tuned mass damper and (b) a tuned liquid column damper. Introduction of the TMD produces a larger index of diagonality, $\rho = 1.72$, in comparison with $\rho = 1.03$ for the structure with the TLCD. Major results are listed below:

1. the asymptotic method with two corrections terms offers an accurate estimation of the response, while the reference solutions are ob-

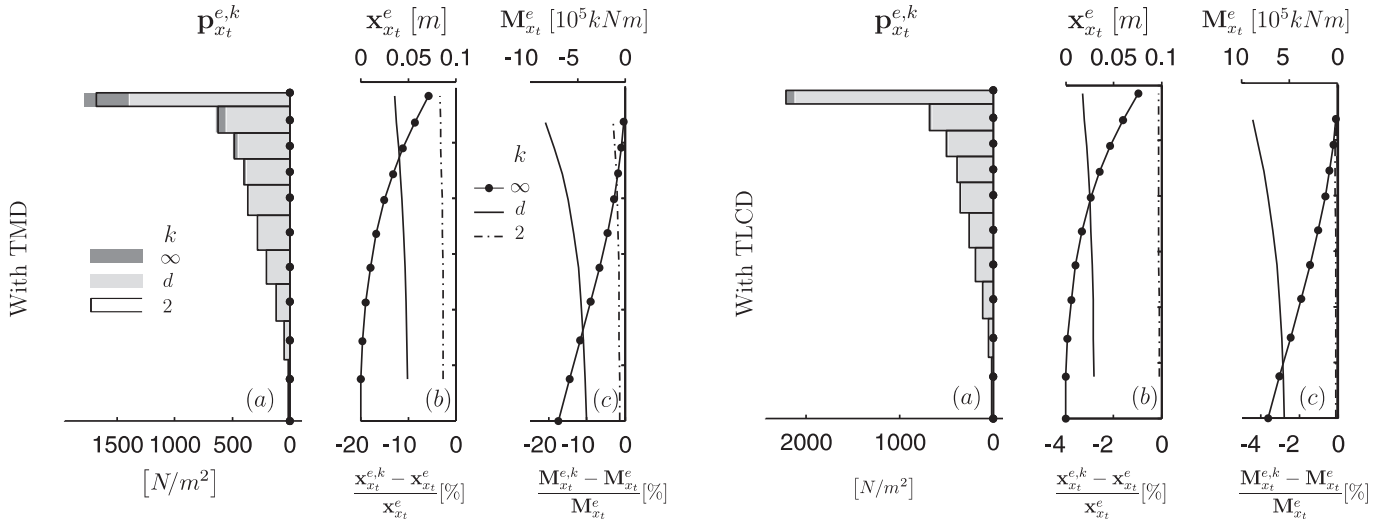

Figure 4: Equivalent static analysis associated with maximisation of the top displacement x_t.(a) Reference equivalent static wind load (grey patch) and those obtained with the decoupling approximation (lighter patch) and the proposed method with second order correction (line). (b) Reference equivalent static displacement and (c) reference equivalent static bending moments. Same conventions of Figure 3 applied for the lower and upper axis.

tained with full inversion of the transfer matrix;

2. expressions of the asymptotic expansion of the weighting coefficients of inertial forces have been derived in order to compute equivalent static wind load;
3. the decoupling approximation can not be stated for the structure with TMD. Indeed, too large underestimations occur for the structural displacements -12% and for the evaluation of the equivalent static wind load. Static analysis produces large underestimations of the static displacements and static bending moments;
4. for the structure with the TLCD, the decoupling approximation may be stated if relative errors smaller than -5% are acceptable. Otherwise, the proposed method with two correction terms produces solutions that are nearly identical to the reference ones;
5. for this structure, peak factors dot not vary significantly between the coupled and uncoupled system;
6. if ESWLs are used for the envelope reconstruction problem (Blaise & Denoël 2013), the decoupling approximation produces large errors on the bending moments under the ESWL that maximizes the top displacement. This justifies the use of the proposed method to ensure reliability when using equivalent static wind loads in a structural design.

REFERENCES

Blaise, N. & V. Denoël (2013). Principal static wind loads. *Journal of Wind Engineering and Industrial Aerodynamics 113*, 29–39.

Canor, T., N. Blaise, & V. Denoël (2012). Efficient uncoupled stochastic analysis with non-proportional damping. *Journal of Sound and Vibration 331*(24), 5283–5291.

Chen, X. Z. & A. Kareem (2001). Equivalent static wind loads for buffeting response of bridges. *Journal of Structural Engineering-Asce 127*(12), 1467–1475.

Clough, R. W. & J. Penzien (1993). *Dynamics of structures* (2nd edition ed.). New-York: McGraw-Hill.

Davenport, A. G. (1961). The application of statistical concepts to the wind loading of structures. *Proceedings of the Institute of Civil Engineers 19*, 449–472.

Davenport, A. G. (1967). Gust loading factors. *In: Proceedings of the American Society of Civil Engineers. Journal of Structural Division 93*(3), 11–34.

Denoël, V. (2009). Estimation of modal correlation coefficients from background and resonant responses. *Structural Engineering And Mechanics 32*(6), 725–740.

Denoël, V. & H. Degée (2009). Asymptotic expansion of slightly coupled modal dynamic transfer functions. *Journal of Sound and Vibration 328*(1-2), 1–8.

Holmes, J. D. (1988). Distribution of peak wind loads on a low-rise building. *Journal Of Wind Engineering and Industrial Aerodynamics 29*(1-3), 59–67.

Holmes, J. D. (1996). Along-wind response of lattice towers - iii. effective load distributions. *Engineering Structures 18*(7), 489–494.

Horn, R. A. & C. R. Johnson (1945). *Matrix Analysis*. Cambridge University Press, Cambridge, United Kingdom.

Kasperski, M. (1992). Extreme wind load distributions for linear and nonlinear design. *Engineering Structures 14*(1), 27–34.

Rayleigh, J. W. S. L. (1877, re-issued 1945). *The Theory of Sound*, Volume 1. New York: Dover Publications.

Rice, S. (1945). Mathematical analysis of random noise. *Bell System Technical Journal 24*, 45–156.

Xu, Y. L., B. Samali, & K. C. S. Kwok (1992). Control of along-wind response of structures by mass and liquid dampers. *J. Engineering Mechanics 118*(1), 20–39.

Zhou, Y., M. Gu, & H. Xiang (1999). Alongwind static equivalent wind loads and responses of tall buildings. part ii: Effects of mode shapes. *Journal of Wind Engineering and Industrial Aerodynamics 79*(1-2), 151–158.